Check for updates

*IET Control Theory & Applications*

WILEY

IET The Institution of Engineering and Technology

ORIGINAL RESEARCH OPEN ACCESS

# Design of Novel Exponential PDN Controller via Quadratic Interpolation Optimiser for Nonlinear and Unstable Ball and Beam System

Davut Izci[1,2] | Serdar Ekinci[3] | Emre Çelik[4] | Murat Uyar[1] | Mohit Bajaj[5,6,7] | Vojtech Blazek[8] | Olena Rubanenko[9]

[1]Department of Electrical and Electronics Engineering, Bursa Uludag University, Bursa, Turkey | [2]Applied Science Research Center, Applied Science Private University, Amman, Jordan | [3]Department of Computer Engineering, Bitlis Eren University, Bitlis, Turkey | [4]Department of Electrical and Electronics Engineering, Düzce University, Düzce, Turkey | [5]Department of Electrical Engineering, Graphic Era (Deemed to Be University), Dehradun, India | [6]Hourani Center for Applied Scientific Research, Al-Ahliyya Amman University, Amman, Jordan | [7]Graphic Era Hill University, Dehradun, India | [8]ENET Centre, CEET, VSB-Technical University of Ostrava, Ostrava, Czech Republic | [9]Department of Power Plants and System, Vinnytsia National Technical University, Vinnytsia, Ukraine

**Correspondence:** Mohit Bajaj (mohitbajajphd@gmail.com) | Olena Rubanenko (olenarubanenko@vntu.edu.ua)

**Received:** 15 September 2025 | **Revised:** 25 November 2025 | **Accepted:** 26 December 2025

## ABSTRACT

This study presents a novel exponential proportional-derivative controller with filter (exp-PDN) for stabilising the nonlinear and underactuated ball and beam system. Unlike conventional PID-based approaches, the proposed controller removes the integral term, resulting in faster transient responses and improved robustness. It incorporates nonlinear exponential shaping of both the error and its derivative, along with a filtered derivative path for enhanced noise handling. A custom multi-objective cost function, comprising the squared error, settling time, and percent overshoot, is proposed to evaluate control performance. The quadratic interpolation optimiser (QIO), a recently developed metaheuristic based on analytical interpolation, is employed to optimise the controller parameters. To validate its effectiveness, the exp-PDN controller is compared against five state-of-the-art metaheuristic algorithms: QIO, spider wasp optimiser, komodo mlipir algorithm, golden eagle optimiser, and slime mould algorithm. The QIO-optimised exp-PDN achieves the best performance, with the lowest cost value (0.3211), minimal overshoot (5.52%), fast rise time (0.97 s), and smallest steady-state error ($4.1643 \times 10^{-4}$). Further comparisons with QIO-optimised phase-lead and PID-with-filter controllers demonstrate the superiority of the proposed method in both transient and steady-state behaviour. In summary, this work advances the control of nonlinear unstable systems by delivering a structurally simple yet highly responsive control architecture. The combination of dual-channel exponential shaping and efficient metaheuristic optimisation results in state-of-the-art closed-loop performance, highlighting the practical value of the proposed exp-PDN framework for real-world control applications.

## 1 | Introduction

The ball and beam system (BBS) has long served as a benchmark model in control engineering due to its underactuated, nonlinear, and inherently unstable nature [1]. Its dynamic behaviour requires the coordination of a single input (beam angle) to control an independent state variable (ball position), making it an ideal testbed for validating the robustness, responsiveness, and adaptability of control strategies. Despite its mechanical simplicity, the BBS presents rich control challenges that demand

This is an open access article under the terms of the Creative Commons Attribution License, which permits use, distribution and reproduction in any medium, provided the original work is properly cited.

© 2026 The Author(s). *IET Control Theory & Applications* published by John Wiley & Sons Ltd on behalf of The Institution of Engineering and Technology.

both precision and flexibility in controller design. It is also worth noting that control principles validated on the ball-and-beam system are highly transferable to real-world systems with similar instability and underactuated dynamics, such as robotic manipulators, precision servo platforms, autonomous balancing systems, and mechatronic positioning devices used in manufacturing. Therefore, improving the performance and implementation efficiency of such benchmark controllers directly supports practical advancements in modern control engineering.

Over the years, researchers have explored a wide range of control methods for stabilising the BBS and improving its performance. Early efforts focused on conventional PID controllers, often optimised using heuristic techniques like particle swarm optimisation (PSO) to improve response characteristics [2]. As control demands grew more complex, hybrid methods combining fuzzy logic and sliding mode control emerged, paired with nature-inspired optimisation algorithms of ant colony optimisation [3]. These approaches offered greater robustness but introduced tuning complexity and parameter sensitivity.

Nonlinear techniques such as backstepping control [4] and coefficient diagram methods (CDM) [5] were also applied to the BBS, delivering improved stability in some cases but often lacking in fast convergence or adaptability. Comparative studies highlighted the trade-offs among classical PID controllers, fuzzy controllers, and adaptive strategies [6]. In pursuit of better tracking and noise rejection, fractional-order controllers [7] and active disturbance rejection control (ADRC) schemes [8] gained traction, demonstrating strong steady-state behaviour but requiring detailed modelling and careful gain selection.

In addition to ball and beam systems, PID-based control strategies remain a preferred choice for stabilising other industrially relevant unstable processes due to their simplicity and practical feasibility. Recent efforts have enhanced PID performance through advanced optimisation and dual-loop formulations to handle severe nonlinearity, ramp tracking, and dead-time behaviour observed in chemical reactors, boiler dynamics, and bioreactors. For instance, robust Smith-predictor-based PID frameworks have been proposed for delay-dominant integrating-type chemical processes to improve disturbance rejection and servo performance [9]. Studies have also examined fractional modified optimal PID and MRAC-assisted FOPID schemes for unstable first-order plus dead-time (FOPTD) and reactor systems, achieving faster convergence and reduced oscillations [10, 11].

Furthermore, dual-loop PID structures have demonstrated strong tracking and regulation capabilities under ramp-type disturbances for unstable CSTRs [12]. Robust I-PD controllers with metaheuristic and stability-guided tuning have shown advantages in noisy and inverse-response environments [13]. Similar advances have also been reported in cascade + feedforward PID designs developed for highly nonlinear Maglev systems, markedly enhancing transient response and noise resilience [14]. The continued prominence of PID-based strategies across nonlinear and unstable industrial applications is also reflected in recent comprehensive surveys and book chapters [15, 16].

Further advancements explored robust control approaches, such as $H\infty$ loop shaping [17], observer-based adaptive fuzzy sliding mode control [18], and state feedback methods tailored to uncertain environments [19]. More recently, interest has turned towards optimisation-augmented fuzzy PID controllers [20], teaching–learning-based PID tuning frameworks [1], and bio-inspired algorithms like the sea lion optimiser within synergetic control systems [21].

While each of these methods brings valuable insights, a recurring theme across the literature is the need for control frameworks that strike a balance between simplicity, adaptability, and robust performance, particularly when addressing the nonlinear and time-varying nature of systems [22] like the BBS. In response to this ongoing challenge, this paper proposes a novel exponential proportional-derivative controller with filter coefficient (exp-PDN). Unlike conventional PID-based designs, the exp-PDN controller deliberately omits the integral component to prevent sluggishness and overshoot associated with integrator windup. Instead, it introduces nonlinear exponential shaping [23] applied to both the error and its derivative, effectively allowing the controller to modulate its aggressiveness in real-time. Additionally, the inclusion of a filter coefficient in the derivative path helps mitigate sensitivity to measurement noise [24], an important consideration in physical implementations.

To fine-tune the controller's parameters, this study employs the quadratic interpolation optimiser (QIO) [25], a recently developed metaheuristic algorithm that estimates minimisers analytically via generalised quadratic interpolation. This approach offers both convergence speed and search precision without the complexity of gradient-based methods. Its efficiency has so far been demonstrated on several different engineering problems [26–30], making it a good candidate for the tuning process of the controller.

Based on these developments, at the heart of this work lies the introduction of a structurally simple yet highly effective exp-PDN, which is a novel control architecture specifically designed for nonlinear and underactuated systems such as the ball and beam. To systematically tune the controller's parameters, a custom multi-objective cost function is developed. This function reflects critical time-domain performance goals, integrating the squared tracking error, settling time, and percent overshoot into a unified evaluation index. The QIO is employed to solve this complex tuning problem.

The effectiveness of the proposed approach is rigorously validated through an extensive suite of simulations and comparisons. Five metaheuristic algorithms (QIO, spider wasp optimiser, komodo mlipir algorithm, golden eagle optimiser, and slime mould algorithm) are benchmarked in terms of statistical consistency, convergence speed, step response dynamics, and error minimisation. Among these, the QIO-optimised exp-PDN controller consistently outperforms its peers, achieving the lowest cost value of 0.3211, a fast rise time of 0.9724 s, a short settling time of 7.5407 s, a minimal overshoot of 5.52%, and the smallest steady-state error of $4.1643\times10^{-4}$. Furthermore, to provide a fair baseline, two classical controllers (a phase-lead compensator and a PID controller with filtered derivative action) were also optimised using the QIO and tested under the same simulation conditions. Even in this extended comparison, the proposed exp-PDN design exhibited superior tracking performance, better



17518652, 2026, 1, Downloaded from https://ietresearch.onlinelibrary.wiley.com/doi/10.1049/cth2.70107 by Turkey Cochrane Evidence Aid, Wiley Online Library on [12/01/2026]. See the Terms and Conditions (https://onlinelibrary.wiley.com/terms-and-conditions) on Wiley Online Library for rules of use; OA articles are governed by the applicable Creative Commons License

disturbance rejection, and stronger robustness across all key metrics.

While many existing approaches, such as PID/FOPID control, sliding-mode control, robust $H\infty$ techniques, and adaptive fuzzy schemes, have demonstrated their capability for stabilising the ball and beam system, they frequently rely on complex-structured controllers, integral compensation, or heavy parameterisation to ensure reliable tracking. In contrast, the proposed exp-PDN controller achieves state-of-the-art closed-loop performance with a structurally simpler formulation by removing the integral term and employing a dual-exponential error-shaping mechanism. This design suppresses integrator-induced overshoot and windup while retaining rapid correction during large deviations, leading to shorter settling times and reduced oscillations compared to classical or fuzzy-based alternatives. Furthermore, the filtered derivative channel ensures robustness to measurement noise, a critical factor for real hardware. The integration of QIO further improves closed-loop behaviour by enabling efficient exploration of the nonlinear parameter space with consistently superior convergence characteristics. Therefore, the proposed framework advances current practice by delivering higher control precision with reduced structural and computational complexity, making it highly relevant for both academic benchmark studies and practical embedded applications.

In light of the discussion presented so far, the main contributions of this study are summarised as follows:

- Proposal of a structurally simplified and computationally efficient nonlinear control design (exp-PDN) for stabilising underactuated and nonlinear systems.
- Integration of exponential nonlinear mapping and filtered derivative action, enabling adaptive and noise-robust control without integral compensation.
- Formulation of a novel multi-objective cost function that simultaneously minimises settling time and overshoot, which are key factors in closed-loop control quality.
- Adoption and application of the QIO for controller tuning, showing superior convergence and solution quality compared to four contemporary algorithms.
- Comprehensive performance validation, including statistical analysis, convergence evolution, time-domain responses, and error-based metrics, clearly demonstrating the superiority of the proposed method.
- Benchmarking against classical control architectures (phase-lead compensator and PID with filter) under identical optimisation setups, highlighting the flexibility and effectiveness of the exp-PDN framework.

The remainder of the paper is organised as follows. Section 2 provides a detailed overview of the QIO, including its exploration-exploitation dynamics and interpolation strategy. Section 3 presents the nonlinear modelling of the ball and beam system, derived using the Lagrangian method and followed by its linearised transfer function. Section 4 introduces the proposed exp-PDN controller, details its mathematical formulation, and explains the application of QIO to optimise its parameters. Section 5 discusses simulation results, including statistical comparisons, cost function evolution, time-domain responses, and controller benchmarking. Finally, Section 6 concludes the paper with a summary of key findings and outlines possible directions for future research.

## 2 | Overview of Quadratic Interpolation Optimiser

The quadratic interpolation optimizer (QIO) is a population-based metaheuristic algorithm designed to balance global exploration and local exploitation by leveraging the mathematical principles of quadratic interpolation [25]. The method operates by estimating the minimum of a fitness function using a quadratic polynomial fitted over three sampled points. These interpolated minima guide the update of candidate solutions towards optimal regions in the search space. As illustrated in Figure 1, the algorithm starts by initialising control parameters such as the population size, the maximum number of iterations, and the weights that govern exploration and exploitation. Once the population is randomly generated, the fitness value $f(x)$ of each individual is evaluated.

### 2.1 | Generalised Quadratic Interpolation

At the core of QIO lies the quadratic interpolation model, defined as:

$$L\ (x) = \alpha^2 + \beta x + \delta \tag{1}$$

where $\alpha, \beta, \delta \in R$ are coefficients determined using three points:

$$\begin{aligned} P_i &= (x_i, f\ (x_i)) \\ P_j &= \left(x_j, f\ \left(x_j\right)\right) \\ P_k &= (x_k, f\ (x_k)) \end{aligned} \tag{2}$$

Given the interpolation conditions:

$$\begin{aligned} (x_i) &= \alpha {x_i}^2 + \beta x_i + \delta = f\ (x_i) \\ LL\ \left(x_j\right) &= \alpha {x_j}^2 + \beta x_j + \delta = f\ \left(x_j\right) \\ L\ (x_k) &= \alpha {x_k}^2 + \beta x_k + \delta = f\ (x_k) \end{aligned} \tag{3}$$

the minimum of the interpolated polynomial is found by setting its derivative to zero:

$$x^* = -\frac{\beta}{2\alpha} \tag{4}$$

The coefficients $\alpha$ and $\beta$ are derived as:

$$\alpha = \frac{\left(x_j - x_k\right) f\ (x_i) + (x_k - x_i) f\ \left(x_j\right) + \left(x_i - x_j\right) f\ (x_k)}{\left(x_j - x_k\right)(x_k - x_i)\left(x_i - x_j\right)} \tag{5}$$

$$\beta = -\frac{\left(x_j^2 - x_k^2\right) f\ (x_i) + \left(x_k^2 - x_i^2\right) f\ \left(x_j\right) + \left(x_i^2 - x_j^2\right) f\ (x_k)}{\left(x_j - x_k\right)(x_k - x_i)\left(x_i - x_j\right)} \tag{6}$$



17518652, 2026, 1, Downloaded from https://ietresearch.onlinelibrary.wiley.com/doi/10.1049/cth2.70107 by Turkey Cochrane Evidence Aid, Wiley Online Library on [12/01/2026]. See the Terms and Conditions (https://onlinelibrary.wiley.com/terms-and-conditions) on Wiley Online Library for rules of use; OA articles are governed by the applicable Creative Commons License

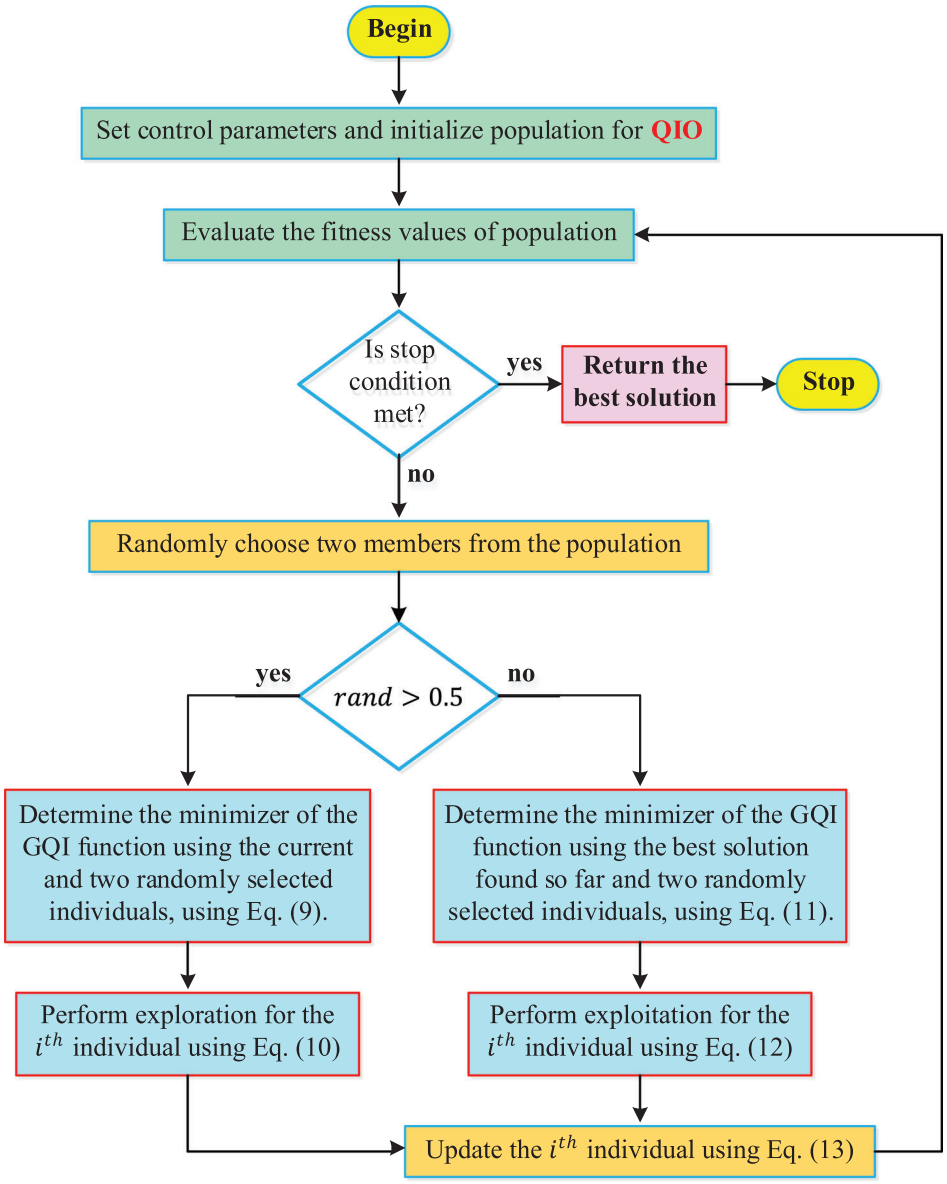



**FIGURE 1** | Flowchart of QIO.

Substituting these into Equation (4), the explicit minimiser becomes:

$$x^* = -\frac{\left(x_j^2 - x_k^2\right) f(x_i) + \left(x_k^2 - x_i^2\right) f(x_j) + \left(x_i^2 - x_j^2\right) f(x_k)}{2 \cdot \left[\left(x_j - x_k\right) f(x_i) + \left(x_k - x_i\right) f(x_j) + \left(x_i - x_j\right) f(x_k)\right]} \tag{7}$$

The full interpolation polynomial is also represented in its Lagrange form as:

$$L(x) = \frac{(x - x_j)(x - x_k)}{(x_i - x_j)(x_i - x_k)} f(x_i) + \frac{(x - x_i)(x - x_k)}{(x_j - x_i)(x_j - x_k)} f(x_j) + \frac{(x - x_i)(x - x_j)}{(x_k - x_i)(x_k - x_j)} f(x_k) \tag{8}$$

This formulation, referred to as generalised quadratic interpolation (GQI), is employed repeatedly throughout the QIO algorithm.

## 2.2 | Main Loop: Exploration and Exploitation

After evaluating the population, the algorithm checks whether the stopping condition has been met. If not, it proceeds to randomly select two individuals from the population for use in either exploration or exploitation. A random number is drawn to decide the direction of search. If $rand > 0.5$, the exploration phase is triggered. In this phase, the minimiser of the GQI function is computed using the current individual and two randomly chosen individuals:

$$x^*_{i,rand1,rand2}(t) = GQI(x_i(t), x_{rand1}(t), x_{rand2}(t), f(x_i(t)), f(x_{rand1}(t)), f(x_{rand2}(t))) \tag{9}$$



17518652, 2026, 1, Downloaded from https://ietresearch.onlinelibrary.wiley.com/doi/10.1049/cth2.70107 by Turkey Cochrane Evidence Aid, Wiley Online Library on [12/01/2026]. See the Terms and Conditions (https://onlinelibrary.wiley.com/terms-and-conditions) on Wiley Online Library for rules of use; OA articles are governed by the applicable Creative Commons License

This minimiser guides the generation of a new exploratory candidate solution as:

$$v_i\ (t+1) = x^*_{i,rand1,rand2}\ (t) + w_1 * \left(x_{rand3}\,(t) - x^*_{i,rand1,rand2}\,(t)\right) + round\,(0.5 * (0.05 + r_1)) * log\frac{r_2}{r_3} \tag{10}$$

Here, $w_1$ is a control weight promoting exploration, and $r_1, r_2, r_3 \in (0,1)$ are random numbers that introduce controlled stochasticity into the movement. Alternatively, if $rand \leq 0.5$, the algorithm switches to exploitation, focusing on refining the best solution obtained so far. In this case, the GQI function is formed using the best solution and two randomly selected individuals:

$$x^*_{best,rand1,rand2}\ (t) = GQI(x_{best}\,(t), x_{rand1}\,(t), x_{rand2}\,(t), f\,(x_{best}\,(t)), f\,(x_{rand1}\,(t)), f\,(x_{rand2}\,(t)) \tag{11}$$

The exploitation update rule is defined as:

$$v_i\ (t+1) = x^*_{best,rand1,rand2}\ (t) + w_2\,.\,(x_{best}\,(t) - round(1+rand)) \cdot \left(\frac{Ub - Lb}{Ub^{rD} - Lb^{rD}}\right).\, x_i^{rD}\,(t) \tag{12}$$

Here, $w_2$ is a control parameter for exploitation, $Ub$ and $Lb$ are the upper and lower bounds of the search space, $rD$ denotes a randomly selected dimension index, and $x_i^{rD}$ is the $rD^{th}$ component of the $i^{th}$ individual. This step focuses on intensifying the search around the most promising regions discovered.

### 2.3 | Position Update and Termination

Following the generation of $v_i(t+1)$, the algorithm performs a greedy update for the $i^{th}$ individual based on the comparison of fitness values:

$$x_i\ (t+1) = \begin{cases} x_i\,(t)\,; f\,(x_i\,(t)) \leq f\,(v_i\,(t+1)) \\ v_i\,(t+1)\,; f\,(x_i\,(t)) > f\,(v_i\,(t+1)) \end{cases} \tag{13}$$

This rule ensures that individuals either improve or maintain their performance in the population. The iterative loop continues until the stopping condition is satisfied. At termination, the best solution found during the run is returned as the final result. This process enables QIO to effectively navigate complex search landscapes by combining the precision of interpolation-based modelling with the robustness of evolutionary population dynamics.

## 3 | Nonlinear Modelling of Ball and Beam System

The ball and beam system (BBS) serves as a canonical example in control theory due to its inherently unstable and nonlinear nature [31]. It is widely utilised to benchmark control strategies, particularly those targeting precision stabilisation of underactuated systems. A schematic representation of the BBS is provided in Figure 2, where the system comprises a beam of length $L$, pivoted at one end, and a ball of mass $m$ and radius $R$ that rolls along the beam. The beam's inclination is governed by a servo-controlled lever arm connected to a rotating gear. The gear rotates by an angle $\theta$, which in turn adjusts the beam angle $\beta$. As the beam tilts, gravitational forces cause the ball to move along its surface. The primary objective of this system is to regulate the beam angle such that the ball maintains a desired position $x$ along the beam.

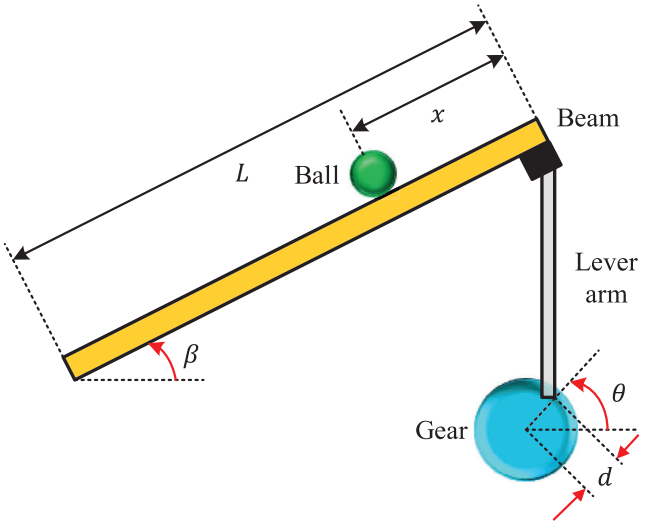



**FIGURE 2** | Illustrative system diagram of BBS.

To mathematically describe the system's dynamics, we employ the Lagrangian formulation, which accounts for both kinetic and potential energy contributions. The resulting nonlinear equation of motion for the ball is expressed as:

$$\left(\frac{J}{R^2} + m\right)\ddot{x} - m x \dot{\beta}^2 + mg\,\sin\beta = 0 \tag{14}$$

Here, $J$ represents the moment of inertia of the ball, $g$ is the gravitational acceleration, and $\beta$ is the instantaneous angle of the beam. For small angular displacements (a common assumption for linear analysis), we approximate $\sin\beta = \beta$, yielding the linearised form:

$$\left(\frac{J}{R^2} + m\right)\ddot{x} + mg\beta = 0 \tag{15}$$

where the beam angle $\beta$ is related to the gear rotation angle $\theta$ through the lever arm geometry, where $d$ denotes the distance from the gear pivot to the beam attachment point:

$$\beta = \frac{d}{L}\,\theta \tag{16}$$

Substituting Equation (16) into the linearised model of Equation (15), we obtain:

$$\left(\frac{J}{R^2} + m\right)\ddot{x} + mg\frac{d}{L}\theta = 0 \tag{17}$$

Applying the Laplace transform under zero initial conditions, we derive the transfer function from the gear angle $\Theta(s)$ to the ball position $X(s)$ as:

$$G\ (s) = \frac{X\,(s)}{\Theta\,(s)} = -\frac{mgd}{L\left(\frac{J}{R^2} + m\right)s^2} \tag{18}$$



17518652, 2026, 1, Downloaded from https://ietresearch.onlinelibrary.wiley.com/doi/10.1049/cth2.70107 by Turkey Cochrane Evidence Aid, Wiley Online Library on [12/01/2026]. See the Terms and Conditions (https://onlinelibrary.wiley.com/terms-and-conditions) on Wiley Online Library for rules of use; OA articles are governed by the applicable Creative Commons License

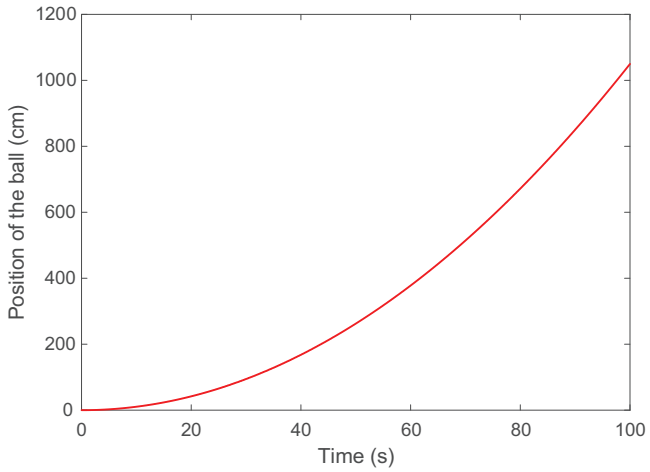



**FIGURE 3** | Step response of open-loop system.

To obtain a concrete form of the transfer function, we substitute the following system parameters, drawn from [6]:

- $m = 0.111$ kg (mass of the ball)
- $R = 0.015$ m (radius of the ball)
- $g = -9.8$ m/s$^2$ (gravitational acceleration)
- $L = 1.0$ m (beam length)
- $d = 0.03$ m (lever arm offset)
- $J = 9.99 \times 10^{-6}\ kg \times m^2$ (moment of inertia)

Using these values, the transfer function simplifies to:

$$G\ (s) = \frac{X\,(s)}{\Theta\,(s)} = \frac{0.21}{s^2} \tag{19}$$

This second-order transfer function highlights the open-loop instability of the system, which is confirmed by the time-domain response shown in Figure 3. The ball's position diverges quadratically over time in response to a step input, indicating that without feedback, the ball cannot be maintained at a stable position. The derived model and transfer function form a foundational basis for developing robust control strategies aimed at stabilising the ball's position through precise manipulation of the beam angle.

## 4 | Development of a Metaheuristic-Driven Novel Control Framework

### 4.1 | Concept of Proposed Controller: Exponential Proportional-derivative With Filter Coefficient

Modern control systems often require fast, non-oscillatory responses while maintaining structural simplicity for practical deployment [23]. In this spirit, we introduce a novel exponential proportional-derivative with filter (exp-PDN) controller, as depicted in Figure 4, which offers nonlinear gain modulation based on error dynamics, without relying on integral action. This design is particularly well-suited for underactuated systems such as the ball and beam, where quick and stable convergence is preferred over integral compensation.

The controller operates by applying nonlinear exponential shaping to both the error signal $e(t)$ and its derivative $\dot{e}(t)$. These signals are first scaled by tunable parameters $\tau_1$ and $\tau_2$, yielding $n\,(t) = e(t) \cdot \tau_1(t)$ and $m\,(t) = \dot{e}\,(t) \cdot \tau_2(t)$. Next, they are passed through the nonlinear exponential mapping function, defined as:

$$f_{exp}\ (u\,(t)) = \left(\frac{1 - e^{-u(t)}}{1 + e^{-u(t)}}\right) \tag{20}$$

This function provides a smooth and symmetric nonlinear transformation, yielding:

$$\begin{aligned} \delta_1\ (t) &= G_1\ \cdot f_{exp}\,(n\,(t)) \\ \delta_2\ (t) &= G_2\ \cdot f_{exp}\,(m\,(t)) \end{aligned} \tag{21}$$

where $G_1$ and $G_2$ are gain coefficients that scale the respective outputs. The final composite signal $\delta(t)$, which serves as the input to the PDN controller, is given by $\delta\ (t) = \delta_1\ (t) + \delta_2\ (t) = G_1\ \cdot f_{exp}(n(t)) + G_2 \cdot f_{exp}(m(t))$.

Unlike traditional PID controllers, the proposed exp-PDN controller does not include an integral term. Instead, it combines proportional and filtered derivative responses based on the nonlinear signal $\delta(t)$. The control signal is defined as:

$$\dot{u}\,(t) + N \cdot u\ (t) = (K_P + K_D \cdot N)\,\dot{\delta}\,(t) + K_P \cdot N \cdot \delta\,(t) \tag{22}$$

where $K_P$ is the proportional gain, $K_D$ is the derivative gain, and $N$ the filter coefficient. This formulation allows for aggressive correction when the system deviates significantly, while attenuating the control action near the setpoint to avoid overshoots or chattering.

The proposed exp-PDN controller offers several distinct advantages that contribute to its effectiveness and practicality. First, by omitting the integral component, the controller achieves faster response times and avoids the slow transient buildup typically associated with integral action. Second, the inclusion of exponential nonlinear mapping allows for dynamic shaping of the control signal based on both the magnitude and rate of the error, improving responsiveness across a wide range of operating conditions. Third, the controller exhibits an inherently time-varying behaviour, adjusting its aggressiveness in real time without the need for external adaptation mechanisms. Last, the integration of a filter coefficient in the derivative path ensures robust noise attenuation, making the controller well-suited for real-world applications where measurement disturbances are common. In the context of the above presentation, the core novelty of the proposed controller lies in the unique combination of three distinct elements. The first one is the omission of the integral term to prevent integrator windup and reduce response delay. The second one is the application of dual nonlinear exponential shaping independently to both the error and its derivative, allowing dynamic gain modulation based on instantaneous signal magnitudes, and the last one is the integration of a filter coefficient in the derivative path for enhanced noise robustness.

While exponential shaping has been investigated in prior studies, existing schemes often apply it only to the error signal or embed it within conventional PID frameworks. In contrast, the exp-PDN



17518652, 2026, 1, Downloaded from https://ietresearch.onlinelibrary.wiley.com/doi/10.1049/cth2.70107 by Turkey Cochrane Evidence Aid, Wiley Online Library on [12/01/2026]. See the Terms and Conditions (https://onlinelibrary.wiley.com/terms-and-conditions) on Wiley Online Library for rules of use; OA articles are governed by the applicable Creative Commons License

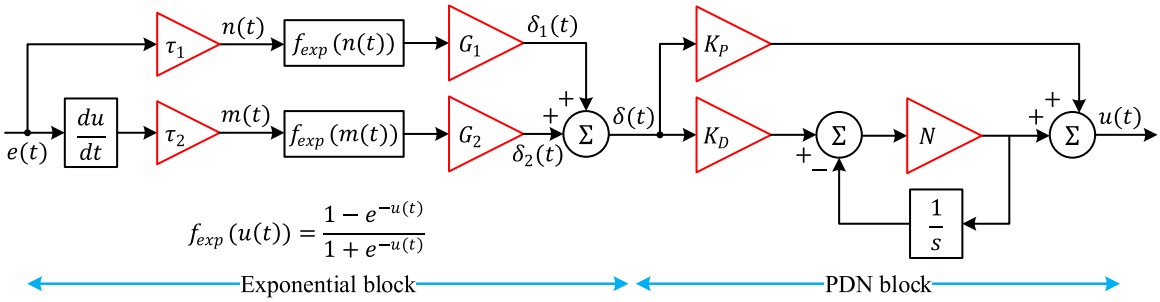



**FIGURE 4** | Block diagram of proposed exp-PDN controller.

controller omits the integral component entirely and introduces symmetric exponential transformation on both input channels. This results in a controller that is structurally lightweight, robust against noise, and capable of adapting its control aggressiveness in real time. Moreover, unlike adaptive or fuzzy-based nonlinear control strategies that rely on complex rule-based systems or switching behaviour, the exp-PDN controller shapes the control action dynamically based on continuously evolving error signals. This design allows the controller to remain aggressive during large deviations and behave conservatively near the desired setpoint without external adaptation mechanisms. To the best of our knowledge, such a synthesis of symmetrical dual-channel exponential modulation, filtered derivative action, and complete removal of the integral term (optimised via a metaheuristic strategy) has not been previously reported for nonlinear and underactuated systems such as the ball and beam. This unique structural and functional synergy constitutes the primary innovation of the proposed exp-PDN controller framework.

### 4.2 | Cost Function and Application of QIO Algorithm to BBS

To achieve optimal performance of the proposed exp-PDN controller on the inherently unstable BBS, the QIO is employed as a metaheuristic parameter tuning strategy. This section outlines the construction of the cost function used for optimisation and explains how the QIO is applied within the control loop. The cost function ($F_{cost}$) is designed to reflect key time-domain performance metrics of the closed-loop system, combining both transient and steady-state behaviours. Specifically, the cost function $F_{cost}$ is expressed as:

$$F_{cost} = (1 - \sigma_1 - \sigma_2) \times \int_0^{t_{sim}} te^2(t)\,dt + \sigma_1 \times t_{set} + \sigma_2 \times p_{os} \quad (23)$$

where $e(t)$ is instantaneous tracking error between the reference input and the system output, $t_{sim}$ is the total simulation time ($t_{sim} = 50$), $t_{set}$ is settling time defined as the time required for the output to remain within ±2% tolerance band around the reference, $p_{os}$ is percent overshoot representing the peak deviation relative to the final value, and $\sigma_1$, $\sigma_2$ ($\sigma_1 = \sigma_2 = 0.01$) are weighting coefficients to prioritise certain aspects of performance during optimisation. This multi-objective structure allows the optimiser to minimise both error energy and undesirable dynamic characteristics, such as long settling times and excessive overshoot.

**TABLE 1** | Constraints of exp-PDN controller for BBS optimization problem.

| Constraint | $K_P$ | $K_D$ | $N$ | $\tau_1$ | $G_1$ | $\tau_2$ | $G_2$ |
|---|---|---|---|---|---|---|---|
| Minimum | 0.1 | 1 | 1 | 1 | 0.1 | 1 | 0.1 |
| Maximum | 2 | 10 | 10 | 20 | 1 | 20 | 1 |

To ensure both performance and feasibility, constraints are imposed on the exp-PDN controller parameters. These bounds define the allowable search space for the optimiser. Table 1 summarises the minimum and maximum limits for each parameter involved in the tuning process. These parameters govern the shape, responsiveness, and stability behaviour of the nonlinear controller. By setting meaningful bounds, the search process is kept focused and physically relevant. In this study, these values were determined based on extensive trial-and-error evaluations.

The integration of the QIO into the BBS control framework is illustrated in Figure 5. At each iteration, QIO generates candidate solutions (i.e., sets of controller parameters), evaluates their performance using the defined cost function, and updates the search based on the generalised quadratic interpolation principle. This optimisation process continues until the maximum number of iterations is reached. The best-performing parameter set is then selected and used to configure the final exp-PDN controller implementation. By leveraging QIO's ability to adaptively explore and exploit the parameter space, the tuning process avoids premature convergence and yields a highly responsive controller. The resulting control strategy demonstrates a robust trade-off between rapid stabilisation, minimal overshoot, and low steady-state error.

## 5 | Simulation Results and Discussion

All simulations in this study were conducted using MATLAB Simulink R2025a on a machine equipped with a 12th Gen Intel Core i7-1260P processor running at 2.10 GHz and 16.0 GB RAM. The simulations employed a fixed-step ODE 4 (Runge-Kutta) solver with a sampling time of 0.01 s, ensuring an adequate trade-off between resolution and computational efficiency for the nonlinear ball and beam system. The implementation of the quadratic interpolation optimiser was performed using MATLAB



17518652, 2026, 1, Downloaded from https://ietresearch.onlinelibrary.wiley.com/doi/10.1049/cth2.70107 by Turkey Cochrane Evidence Aid, Wiley Online Library on [12/01/2026]. See the Terms and Conditions (https://onlinelibrary.wiley.com/terms-and-conditions) on Wiley Online Library for rules of use; OA articles are governed by the applicable Creative Commons License

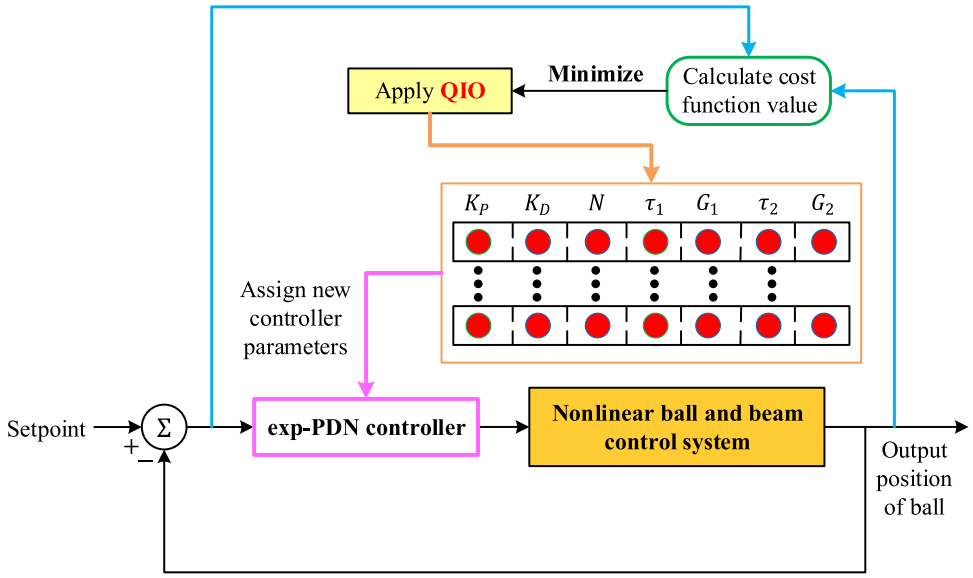



**FIGURE 5** | Integration of QIO in position control for BBS.

scripting, and its source code is publicly available through the MATLAB File Exchange platform, enabling reproducibility and future extensions by interested researchers.

### 5.1 | Selected Metaheuristic Optimisation Methods

To ensure a fair and comprehensive evaluation of the proposed control framework, five distinct metaheuristic optimisation algorithms are employed to tune the parameters of the exp-PDN controller. These algorithms are selected based on their proven capabilities in solving complex, nonlinear, and high-dimensional optimisation problems. The algorithms considered in this study are quadratic interpolation optimiser (QIO) [25], spider wasp optimizer (SWO) [32], komodo mlipir algorithm (KMA) [33], golden eagle optimiser (GEO) [34], and slime mould algorithm (SMA) [35]. Each of these methods adopts a unique nature-inspired or mathematically driven search strategy to explore the solution space.

Although classical algorithms such as particle swarm optimisation (PSO) [36], genetic algorithm (GA) [37], and differential evolution (DE) [38] are well-established in control literature, the selected methods in this study reflect recent advances in the field of metaheuristics. These contemporary algorithms have been shown in the literature to outperform traditional methods in various challenging scenarios by incorporating sophisticated mechanisms for global exploration, local exploitation, and adaptive behaviour. For instance, SMA and SWO utilise dynamic search strategies inspired by biological systems, while GEO and KMA adopt mathematically grounded or nature-inspired models that enable better navigation of complex search landscapes. Their superior convergence characteristics and robustness against local minima make them highly suitable for evaluating modern control strategies.

QIO serves as the primary method for this study due to its interpolation-based minimiser estimation, while the remaining four are benchmarked to validate the relative performance of the proposed optimisation framework. All optimisation algorithms are configured with a common experimental setup to ensure consistency in comparison. Specifically, each method uses a swarm/population size of 25, a maximum of 100 iterations, and 30 independent runs to account for stochastic variability. The detailed parameter settings for each algorithm are summarised in Table 2, ensuring each method is evaluated under its best-practice or recommended configurations. By applying this structured

**TABLE 2** | Setting parameters of optimisation methods.

| Optimisation method | Parameter | Value |
|---|---|---|
| QIO | Swarm size | 25 |
| | Iteration number | 100 |
| SWO | Swarm size | 25 |
| | Iteration number | 100 |
| | Crossover probability | 0.2 |
| | Trade-off probability | 0.3 |
| | Minimum population size | 20 |
| KMA | Swarm size | 25 |
| | Iteration number | 100 |
| | Female mutation radius | 0.5 |
| | Female mutation rate | 0.5 |
| | Mlipir rate | 0.5 |
| GEO | Swarm size | 25 |
| | Iteration number | 100 |
| | Propensity to attack | [0.5, 2] |
| | Propensity to cruise | [1, 0.5] |
| SMA | Swarm size | 25 |
| | Iteration number | 100 |
| | Control parameter $z$ | 0.03 |



17518652, 2026, 1, Downloaded from https://ietresearch.onlinelibrary.wiley.com/doi/10.1049/cth2.70107 by Turkey Cochrane Evidence Aid, Wiley Online Library on [12/01/2026]. See the Terms and Conditions (https://onlinelibrary.wiley.com/terms-and-conditions) on Wiley Online Library for rules of use; OA articles are governed by the applicable Creative Commons License

**TABLE 3** | Comparison of statistical metrics for cost function ($F_{cost}$).

| Statistical metric | QIO | SWO | KMA | GEO | SMA |
|---|---|---|---|---|---|
| Best | 0.3211 | 0.3403 | 0.3813 | 0.3854 | 0.3668 |
| Worst | 0.3720 | 0.3969 | 0.4338 | 0.4388 | 0.4243 |
| Median | 0.3291 | 0.3516 | 0.3964 | 0.4034 | 0.3795 |
| Average | 0.3338 | 0.3573 | 0.4025 | 0.4083 | 0.3873 |
| Standard deviation | 0.0124 | 0.0156 | 0.0167 | 0.0164 | 0.0178 |
| Friedman's mean rank | 1 | 2 | 4 | 5 | 3 |
| $p$-value (Wilcoxon's test) | — | 2.8434E−05 | 1.7344E−06 | 1.7344E−06 | 1.7344E−06 |

and comparative evaluation approach, the effectiveness of QIO in tuning the proposed exp-PDN controller can be directly benchmarked against a diverse set of contemporary algorithms. The results from this multi-algorithm comparison are further discussed in the subsequent subsections, where performance is assessed using statistical analyses, convergence behavior, and closed-loop system responses.

## 5.2 | Statistical Analysis

To assess the performance consistency and robustness of each optimisation method, a statistical analysis was conducted over 30 independent optimisation runs per algorithm. This section compares the statistical behaviour of the five metaheuristic algorithms (QIO, SWO, KMA, GEO, and SMA) using key performance indicators derived from their respective cost function evaluations. Importantly, the controller structure remains identical across all benchmark cases; each implementation uses the same exp-PDN architecture, including the nonlinear exponential shaping and filtered derivative components. The only variation lies in the choice of metaheuristic used to tune the controller parameters. This ensures that any observed performance differences can be attributed solely to the optimiser's effectiveness and not to structural discrepancies in the control design.

A summary of the results is presented in Table 3, including the best, worst, median, average, and standard deviation of the final cost values obtained by each algorithm. Additionally, Friedman's mean rank and Wilcoxon's signed-rank test $p$-values are included to facilitate a rigorous non-parametric comparison of optimisation performance.

The results clearly show that QIO consistently outperforms all other algorithms across every statistical metric. Notably, it achieved the lowest best cost value (0.3211) and maintained a minimal standard deviation (0.0124), highlighting both its effectiveness and robustness. In contrast, algorithms such as KMA and GEO exhibited higher average costs and broader variances, indicating less reliable convergence behaviour. Moreover, the Friedman rank test places QIO in the top position (rank 1), reaffirming its dominance in performance. The Wilcoxon signed-rank test reveals statistically significant differences ($p$-values $<$ 0.05) between QIO and all other methods, thereby validating the superiority of QIO's parameter optimisation strategy from a statistical standpoint. The boxplot visualisation in Figure 6

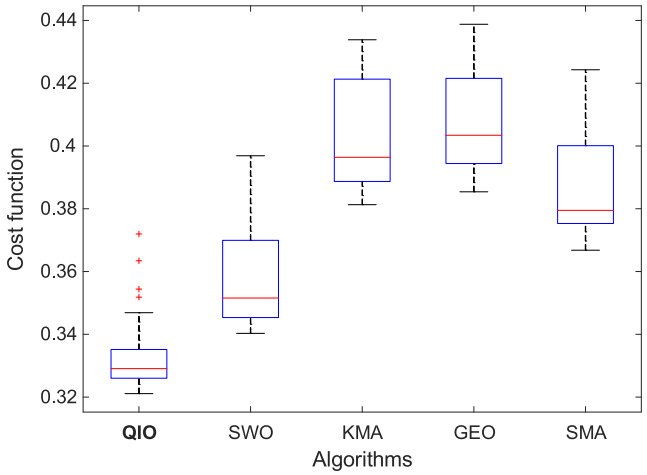



**FIGURE 6** | Boxplot analysis of optimisation methods.

further illustrates the distribution of results from each algorithm. QIO not only exhibits a lower central tendency but also demonstrates tighter interquartile ranges, confirming its superior stability.

## 5.3 | Evolution of Cost Function

To further assess the convergence behaviour and optimisation efficiency of each algorithm, the evolution of the cost function over iterations is examined. This analysis offers valuable insights into how quickly and effectively the optimisation methods explore and exploit the search space to reach high-quality solutions. Figure 7 illustrates the best cost function trajectories for the five metaheuristic algorithms (QIO, SWO, KMA, GEO, and SMA) evaluated over 30 independent runs.

Among all algorithms, the QIO demonstrates the fastest and most stable convergence, reaching a near-optimal solution in significantly fewer iterations. Its curve flattens early, indicating rapid stabilisation around a minimal cost region. This behaviour reflects QIO's strong balance between exploration and exploitation, effectively guiding the search process towards promising areas without excessive wandering. In contrast, the remaining algorithms (particularly KMA and GEO) exhibit slower and more oscillatory convergence patterns. Their cost trajectories



17518652, 2026, 1, Downloaded from https://ietresearch.onlinelibrary.wiley.com/doi/10.1049/cth2.70107 by Turkey Cochrane Evidence Aid, Wiley Online Library on [12/01/2026]. See the Terms and Conditions (https://onlinelibrary.wiley.com/terms-and-conditions) on Wiley Online Library for rules of use; OA articles are governed by the applicable Creative Commons License

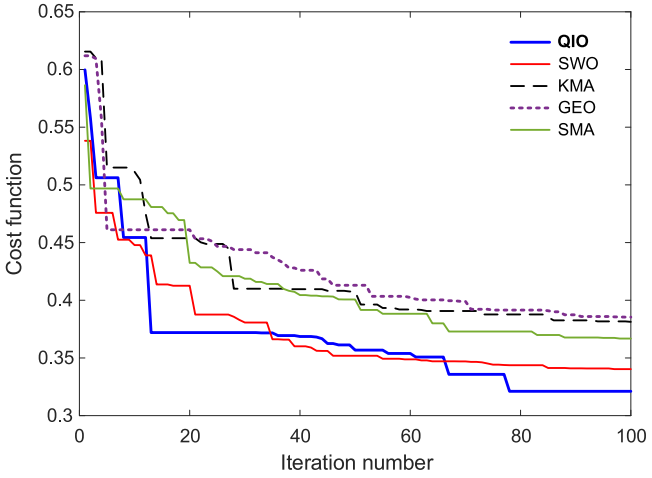



**FIGURE 7** | Change of cost function ($F_{cost}$).

**TABLE 4** | Optimal exp-PDN controller parameters.

| Parameter | QIO | SWO | KMA | GEO | SMA |
|---|---|---|---|---|---|
| $K_P$ | 1.9705 | 1.6772 | 1.4149 | 1.9065 | 1.3466 |
| $K_D$ | 9.6619 | 8.5942 | 7.5380 | 9.1832 | 7.3274 |
| $N$ | 3.3765 | 4.1304 | 5.2302 | 5.1726 | 5.2437 |
| $\tau_1$ | 5.2089 | 5.2789 | 7.3260 | 5.5810 | 7.5105 |
| $G_1$ | 0.9702 | 0.9408 | 0.9412 | 0.9905 | 0.9981 |
| $\tau_2$ | 1.8453 | 1.9863 | 2.6165 | 1.6284 | 1.3839 |
| $G_2$ | 0.7411 | 0.6013 | 0.5341 | 0.8859 | 0.9931 |

continue to decline gradually over time, suggesting either delayed convergence or less precise minimiser estimation. SWO and SMA show moderate convergence speed but fail to match the final accuracy of QIO.

To support the visual observations, Table 4 presents the optimal exp-PDN controller parameters obtained by each optimisation method. These parameters correspond to the best solution found during the 30 independent runs and directly reflect the influence of each optimiser's search capability on controller tuning. These results reinforce the earlier statistical findings: QIO not only converges faster but also delivers more effective controller parameters, contributing to improved dynamic performance of the closed-loop system.

### 5.4 | Step Response of Closed-loop System

To assess the dynamic performance of the proposed exp-PDN controller and compare it against alternative tuning strategies, the step responses of the closed-loop BBS are analysed under parameter sets obtained by each of the five metaheuristic algorithms. The time-domain behaviour is evaluated using key performance metrics such as rise time ($t_{rise}$), settling time ($t_{set}$), percent overshoot ($P_{os}$), and peak time ($t_p$). Figure 8 presents the step responses of the closed-loop system when tuned with QIO, SWO, KMA, GEO, and SMA. A magnified view around the

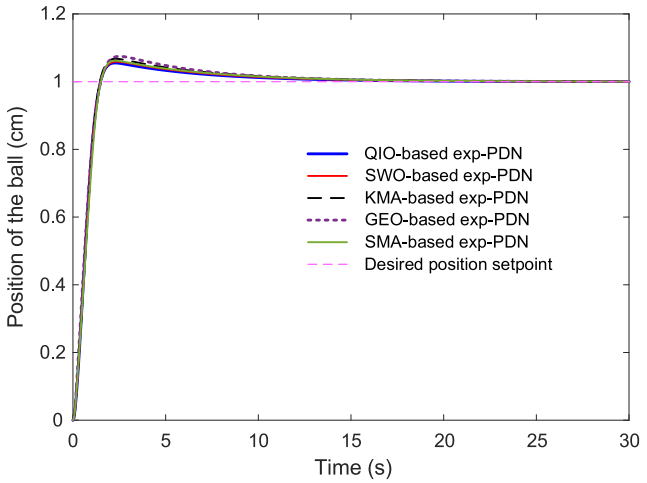



**FIGURE 8** | Step response of exp-PDN controlled closed-loop system.

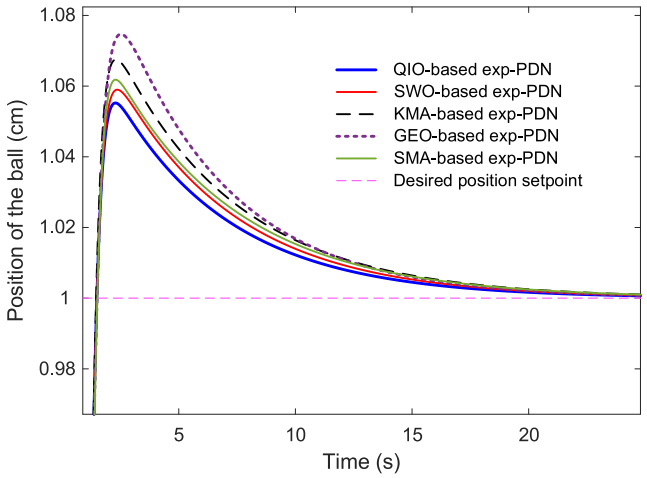



**FIGURE 9** | Enlarged version of Figure 8.

steady-state region is shown in Figure 9 to provide additional clarity in comparing overshoot and settling behaviour. Among all controllers, the QIO-tuned exp-PDN achieves the most desirable response characteristics. It features the fastest rise time (0.9724 s) and a relatively short settling time (7.5407 s). In addition, its percent overshoot is limited to 5.5221%, which is lower than that of all benchmarked algorithms. The smooth trajectory and rapid stabilisation underscore QIO's capability to effectively guide the control parameters towards optimal solutions. By contrast, controllers tuned with KMA and GEO exhibit significantly longer settling times and higher overshoots, indicating suboptimal parameter selection. While SWO and SMA offer moderately competitive results, they fall short of matching QIO's overall performance.

The quantitative comparison is summarised in Table 5, which presents the key stability metrics for each controller configuration. These results clearly indicate that the QIO-optimised controller strikes an effective balance between speed and stability. Its lower overshoot helps mitigate risks of control saturation or oscillation, while its fast response characteristics ensure



17518652, 2026, 1, Downloaded from https://ietresearch.onlinelibrary.wiley.com/doi/10.1049/cth2.70107 by Turkey Cochrane Evidence Aid, Wiley Online Library on [12/01/2026]. See the Terms and Conditions (https://onlinelibrary.wiley.com/terms-and-conditions) on Wiley Online Library for rules of use; OA articles are governed by the applicable Creative Commons License

**TABLE 5** | Comparison of stability **metrics**.

| Stability metric | QIO | SWO | KMA | GEO | SMA |
|---|---|---|---|---|---|
| $t_{rise}$ (s) | 0.9724 | 0.9747 | 0.9780 | 1.0056 | 1.0260 |
| $t_{set}$ (s) | 7.5407 | 8.1539 | 8.9492 | 9.1694 | 8.5546 |
| $p_{os}(\%)$ | 5.5221 | 5.8986 | 6.7521 | 7.4702 | 6.1811 |
| $t_p$ (s) | 2.2800 | 2.3600 | 2.3100 | 2.5200 | 2.2900 |

timely error correction. In conclusion, the step response analysis reaffirms that the QIO-tuned exp-PDN controller delivers superior closed-loop performance, outperforming contemporary metaheuristic methods in terms of responsiveness, smoothness, and stability.

## 5.5 | Error Metrics

In addition to time-domain response characteristics, quantitative evaluation of control performance is further reinforced through error-based performance indices. This section presents a comparative analysis using two widely accepted error metrics: the integral of absolute error (IAE) [39] and the steady-state error ($e_{ss}$) [40]. The IAE is defined as:

$$\text{IAE} = \int_0^{t_{sim}} e(t)\, dt \tag{24}$$

where $e(t)$ represents the instantaneous tracking error between the desired and actual ball positions, and $t_{sim}$ is the total simulation time, set to 50 s in this study. This metric captures the cumulative magnitude of the tracking error, making it sensitive to both transient and steady-state performance. The $e_{ss}$, on the other hand, reflects the absolute value of the residual error at the final moment of simulation. These metrics provide a more precise understanding of how well each controller maintains trajectory accuracy and eliminates error over time. The comparative results are summarised in Table 6. The QIO-optimised controller exhibits the lowest IAE value, indicating superior cumulative error handling over the simulation period. This result aligns with earlier findings related to rapid settling and reduced overshoot. Although GEO achieved a comparable IAE, its steady-state error was higher, indicating weaker final tracking performance. In terms of $e_{ss}$, the QIO-tuned controller also outperformed the alternatives, achieving the smallest residual error at the end of the simulation. Both KMA and GEO showed relatively higher $e_{ss}$ values, suggesting that their solutions struggled with final convergence accuracy. Overall, the error metric analysis confirms that the QIO algorithm not only excels in shaping the dynamic response of the exp-PDN controller but also ensures precise long-term tracking performance.

## 5.6 | Comparison With Various Controller Types

To further evaluate the effectiveness of the proposed exp-PDN controller tuned by the QIO algorithm, its performance is compared against two well-established control structures: the phase-lead compensator and the PID controller with filter. These classical controllers were also tuned using the QIO algorithm to ensure a fair comparison under identical optimisation conditions and system dynamics. The phase-lead compensator is a classical compensator structure known for improving the transient response and enhancing system stability. Its transfer function is given by [41]:

$$C_{lead}\ (s) = K\frac{s+z}{s+p} \tag{25}$$

In this formulation, $K$ denotes the overall gain, $z$ is the zero location, and $p$ is the pole location, with the condition that $p > z$. In practical lead compensator design, the zero and pole are positioned such that the zero lies closer to the origin than the pole on the negative real axis. This configuration ensures that the compensator contributes a net positive phase to the open-loop transfer function, thereby improving system stability and accelerating the transient response. In this study, the optimised parameters by QIO are found as $K = 11.2516$, $z = 0.0661$ and $p = 4.2638$.

On the other hand, the PID controller with filter [42] incorporates a first-order low-pass filter in the derivative path to suppress high-frequency noise, and is expressed as:

$$C_{PID}\ (s) = K_P + \frac{K_I}{s} + K_D\frac{Ns}{s+N} \tag{26}$$

where $K_P$ , $K_I$ , and $K_D$ are the proportional, integral, and derivative gains, respectively, and $N$ is the filter coefficient. In this study, the optimised parameters by QIO are found as $K_P = 0.8487$, $K_I = 0.0016$, $K_D = 5.0915$ and $N = 5.7352$. The optimal parameter values for both controller types were obtained using the QIO, with the same cost function and simulation setup applied to the exp-PDN design.

The step responses of the closed-loop system under each QIO-optimised controller are shown in Figure 10. Visually, the exp-PDN controller offers a markedly superior performance, featuring faster convergence, lower overshoot, and smoother transitions, compared to the phase-lead and filtered PID counterparts.

Quantitative comparison metrics are presented in Table 7, detailing the rise time, settling time, percent overshoot, and peak time for all three controllers. The results highlight the clear performance advantage of the exp-PDN controller in terms of both transient response and stability. Its ability to rapidly stabilise

**TABLE 6** | Comparison of error metrics.

| Error metric | QIO | SWO | KMA | GEO | SMA |
|---|---|---|---|---|---|
| $e_{ss}(\%)$ | 4.1643E−04 | 5.8550E−04 | 9.0892E−04 | 4.1813E−04 | 0.0010 |
| $IAE$ | 1.0023 | 1.0382 | 1.1096 | 1.1033 | 1.0913 |



17518652, 2026, 1, Downloaded from https://ietresearch.onlinelibrary.wiley.com/doi/10.1049/cth2.70107 by Turkey Cochrane Evidence Aid, Wiley Online Library on [12/01/2026]. See the Terms and Conditions (https://onlinelibrary.wiley.com/terms-and-conditions) on Wiley Online Library for rules of use; OA articles are governed by the applicable Creative Commons License

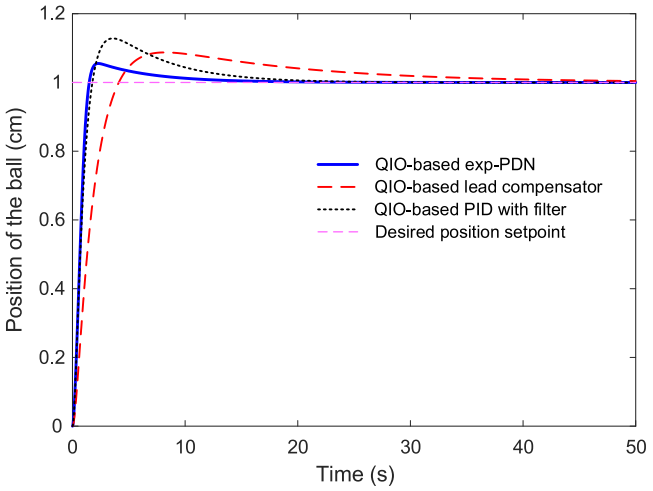



**FIGURE 10** | Step response of closed-loop system optimized by QIO algorithm.

**TABLE 7** | Comparison of stability metrics for QIO-based controllers.

| Stability metric | exp-PDN | Lead compensator | PID with filter |
|---|---|---|---|
| $t_{rise}$ (s) | 0.9724 | 2.6940 | 1.1875 |
| $t_{set}$ (s) | 7.5407 | 29.4111 | 14.0180 |
| $p_{os}$(%) | 5.5221 | 8.7422 | 12.8138 |
| $t_p$ (s) | 2.2800 | 8.2100 | 3.5800 |

**TABLE 8** | Comparison of error metrics for QIO-based controllers.

| Error metric | exp-PDN | Lead compensator | PID with filter |
|---|---|---|---|
| $e_{ss}$(%) | 4.1643E−04 | 0.4143 | 0.0312 |
| IAE | 1.0023 | 3.0299 | 1.6862 |

the system with minimal overshoot makes it highly effective for the nonlinear dynamics of the ball and beam setup (See Table 7).

To complement the time-domain analysis, error-based performance metrics, IAE and $e_{ss}$, are also computed for each controller and summarised in Table 8. The exp-PDN controller again outperforms its counterparts, demonstrating the lowest integral of absolute error and the smallest steady-state error. While the PID with filter controller achieved a modest IAE, its $e_{ss}$ remained significantly higher than that of the exp-PDN design. The phase-lead compensator performed the weakest across both metrics. Overall, the comparative analysis reinforces the strength of the QIO-tuned exp-PDN controller. Its advanced error shaping, nonlinear gain modulation, and filtered derivative action enable it to deliver superior tracking accuracy, fast convergence, and strong robustness, surpassing traditional linear control techniques in handling the nonlinear, underactuated dynamics of the ball and beam system. These findings demonstrate that the proposed QIO-optimised exp-PDN controller not only surpasses four recent metaheuristic-based tuning strategies but also outperforms practically relevant benchmark controllers under identical conditions, confirming its advancement over the current state-of-the-art in ball-and-beam control.

### 5.7 | Discussion on Practical Implementation Considerations

Although the proposed exp-PDN controller is evaluated solely through extensive simulations, it is important to examine its feasibility and implications for real-world implementation. First, it should be emphasised that all simulation results were obtained using the actual nonlinear model of the ball and beam system derived from Lagrangian dynamics. This nonlinear model captures the complex behaviour and instability of the physical system, thereby offering a reliable platform for evaluating control strategies under conditions that closely approximate hardware reality.

From a practical standpoint, the proposed controller structure offers several advantages that favour hardware deployment. The exp-PDN controller is structurally simple, comprising only a nonlinear transformation of the error and a filtered derivative term. Unlike classical PID or adaptive controllers that rely on integral action or complex adaptation laws, the exp-PDN avoids computationally expensive processes, which is beneficial for implementation on real-time embedded platforms such as microcontrollers or DSPs. Moreover, the nonlinear exponential mapping used in the controller is continuous and bounded, which prevents abrupt control actions and mitigates the risk of actuator saturation, which is an important consideration in hardware systems. The inclusion of a filter in the derivative path further enhances robustness by attenuating high-frequency noise, which is often present in sensor signals in practical environments.

Another important practical consideration involves the effect of loop delays and sampling constraints on real-time performance. While this study did not explicitly incorporate such delays into the simulation model, we recognise that they are often unavoidable in embedded implementations. The exp-PDN controller, by design, offers favourable traits for delay-tolerant execution. Its structurally minimal formulation (free from complex adaptation or multi-stage filtering) translates to faster computation and reduced latency on real-time platforms. The inclusion of a filter in the derivative channel also mitigates the impact of high-frequency disturbances, which tend to be amplified in systems with limited sampling resolution. However, it is important to note that large or variable delays can still pose challenges, and formal delay sensitivity analysis remains an area for future investigation. We consider this a meaningful direction for future studies, particularly for implementations involving low-cost hardware or networked control settings.

Regarding the absence of the integral term in the controller structure, we acknowledge that while integral action is traditionally used to eliminate steady-state error, it can introduce performance trade-offs such as increased overshoot or integrator windup. In our design, the omission of the integral component was a deliberate choice aimed at achieving faster transient performance and avoiding issues associated with long-term accumulation of



17518652, 2026, 1, Downloaded from https://ietresearch.onlinelibrary.wiley.com/doi/10.1049/cth2.70107 by Turkey Cochrane Evidence Aid, Wiley Online Library on [12/01/2026]. See the Terms and Conditions (https://onlinelibrary.wiley.com/terms-and-conditions) on Wiley Online Library for rules of use; OA articles are governed by the applicable Creative Commons License

error. Instead, the dual-channel exponential shaping mechanism offers dynamic gain modulation based on instantaneous error and its derivative, which inherently helps in suppressing steady-state deviations. Although this strategy has shown effective steady-state performance in our nonlinear simulations, we recognise that in the presence of persistent disturbances or model mismatches, small residual steady-state errors may still occur. This trade-off has been noted as a potential limitation and may be addressed in future extensions of this work, such as through the integration of disturbance observers or hybrid integral correction mechanisms.

An equally important aspect of practical implementation is the computational overhead associated with the parameter tuning process. The QIO, which was used in this study to optimise the exp-PDN controller parameters, was selected not only for its recent introduction but also for its promising performance in terms of convergence speed and computational efficiency. QIO features a low-complexity structure and minimal memory footprint, making it a strong candidate for control-related optimisation tasks. During experimentation, QIO consistently required lower computational effort compared to other tested metaheuristics under the same conditions, and it demonstrated smooth and reliable convergence trends. These characteristics render QIO particularly well-suited for offline optimisation, where the best-performing parameters can be identified in advance and subsequently deployed in real-time control scenarios. While detailed runtime profiling and complexity analysis were beyond the scope of this work, our experience indicates that QIO offers a favourable balance between optimisation quality and computational load.

Nonetheless, we acknowledge that certain practical challenges may arise during physical implementation. These include sensor calibration errors, actuator backlash, mechanical friction, and time delays in control signal execution. Furthermore, tuning the controller parameters in real-time using QIO or any other metaheuristic method could require considerable computational resources. A potential solution is to perform the optimisation offline and then implement the best-found parameters in a real-time control loop. In summary, the proposed exp-PDN controller, despite being validated in a simulation environment, is both computationally efficient and structurally suitable for real-time deployment. The use of the full nonlinear model in simulations further supports the relevance and transferability of the findings to physical systems.

## 6 | Conclusion

This paper introduced a novel exp-PDN controller, optimised using the QIO, for effective control of the nonlinear and underactuated ball and beam system. The proposed controller eliminates the integral component found in traditional PID structures, instead leveraging exponential nonlinear shaping of the error and its derivative, along with a filtered derivative path. This design enhances transient performance, avoids integrator-induced sluggishness, and ensures robustness against noise and disturbances. A custom cost function, incorporating the squared tracking error, settling time, and percent overshoot, was formulated to reflect both transient and steady-state performance objectives. QIO, selected for its efficient interpolation-based search capability, was used to optimise the exp-PDN controller's parameters. The method was benchmarked against four contemporary metaheuristic algorithms: SWO, KMA, GEO, and SMA. Extensive statistical analyses, cost-evolution studies, and time-domain simulations demonstrated that the QIO-optimised exp-PDN consistently outperformed all competing methods. It achieved the lowest cost value (0.3211), fastest rise time (0.9724 s), shortest settling time (7.5407 s), lowest overshoot (5.52%), and smallest steady-state error ($4.1643 \times 10^{-4}$). Additional comparisons were carried out against QIO-optimised phase-lead compensators and PID-with-filter controllers. The exp-PDN controller proved superior in both transient dynamics and error minimisation, highlighting its adaptability and effectiveness for nonlinear system control. In quantitative terms, the proposed controller achieved up to a 27.31% reduction in settling time and a 42.85% overshoot reduction compared to the best-performing benchmark among the tested metaheuristic-tuned controllers. Against classical QIO-based tuning of the phase-lead and PID-with-filter designs, the exp-PDN provided improvements exceeding 30% in rise-time acceleration and over one order of magnitude reduction in steady-state error, demonstrating its effectiveness not only in transient shaping but also in accuracy and disturbance rejection. These measurable gains clearly validate the performance advantages achieved through the synergistic combination of exponential shaping and efficient parameter optimisation. The structural simplicity of the proposed controller and its reliance on only a proportional and filtered derivative action make it attractive for practical implementation on embedded hardware. The dual exponential shaping enables dynamic modulation of the control aggressiveness without requiring integral compensation or complex adaptation mechanisms, contributing to strong disturbance attenuation and reduced oscillations in the closed-loop response. These characteristics demonstrate meaningful advantages over conventional controllers for unstable nonlinear systems.

Future work may focus on experimental validation using a physical ball and beam laboratory setup, particularly to study real-time effects such as actuator saturation, friction, and sampling delays. Extending the exp-PDN concept to multi-input, multi-output systems or integrating disturbance observers may further enhance steady-state accuracy and robustness. Overall, the results confirm that the proposed controller offers a promising and computationally efficient solution for advanced nonlinear control applications.

### Author Contributions

**Davut Izci**: conceptualisation, methodology, software, visualisation, investigation, writing – original draft preparation. **Serdar Ekinci**: conceptualisation, methodology, software, visualisation, investigation, writing – original draft preparation. **Emre Çelik**: conceptualisation, methodology, software, visualisation, investigation, writing – original draft preparation. **Murat Uyar**: data curation, validation, supervision, resources, writing – review and editing. **Mohit Bajaj**: project administration, funding, supervision, resources, writing – review and editing. **Olena Rubanenko**: project administration, funding, supervision, resources, writing – review and editing. **Vojtech Blazek**: project administration, funding, supervision, resources, writing – review and editing.

### Acknowledgements

This research is funded by European Union under the REFRESH—Research Excellence For Region Sustainability and High-Tech Industries



17518652, 2026, 1, Downloaded from https://ietresearch.onlinelibrary.wiley.com/doi/10.1049/cth2.70107 by Turkey Cochrane Evidence Aid, Wiley Online Library on [12/01/2026]. See the Terms and Conditions (https://onlinelibrary.wiley.com/terms-and-conditions) on Wiley Online Library for rules of use; OA articles are governed by the applicable Creative Commons License

Project via the Operational Programme Just Transition under Grant CZ.10.03.01/00/22_003/0000048; in part by the National Centre for Energy II and ExPEDite Project a Research and Innovation Action to Support the Implementation of the Climate Neutral and Smart Cities Mission Project TN02000025; and in part by ExPEDite through European Union's Horizon Mission Programme under Grant 101139527. The authors would like to express their sincere gratitude to Lukas Prokop and Stanislav Misak for their exceptional supervision, project administration, and overall guidance throughout the course of this project. Their expertise and support were instrumental to its success.

### Conflicts of Interest

The authors declare no conflicts of interest.

### Data Availability Statement

All relevant data are within the manuscript. The collection and analysis method complied with the terms and conditions for the source of the data.

### References

1. S. Chaturvedi, N. Kumar, and R. Kumar, "Two Feedback PID Controllers Tuned With Teaching–Learning-Based Optimization Algorithm for Ball and Beam System," *IETE Journal of Research* 70, no. 7 (2024): 6340–6349, https://doi.org/10.1080/03772063.2023.2284955.

2. M. A. Rana, Z. Usman, and Z. Shareef, "Automatic Control of Ball and Beam System Using Particle Swarm Optimization," in *Proceedings of the 2011 IEEE 12th International Symposium on Computational Intelligence and Informatics* (CINTI), (IEEE, 2011), 529–534.

3. Y.-H. Chang, C.-W. Chang, C.-W. Tao, H.-W. Lin, and J.-S. Taur, "Fuzzy Sliding-mode Control for Ball and Beam System With Fuzzy Ant Colony Optimization," *Expert Systems With Applications* 39, no. 3 (2012): 3624–3633, https://doi.org/10.1016/j.eswa.2011.09.052.

4. A. A. Ezzabi, K. C. Cheok, and F. A. Alazabi, "A Nonlinear Backstepping Control Design for Ball and Beam System," in *Proceedings of the 2013 IEEE 56th International Midwest Symposium on Circuits and Systems (MWSCAS)*, (IEEE, 2013), 1318–1321, https://doi.org/10.1109/MWSCAS.2013.6674898.

5. B. Meenakshipriya and K. Kalpana, "Modelling and Control of Ball and Beam System Using Coefficient Diagram Method (CDM) Based PID Controller," *IFAC Proceedings Volumes* 47, no. 1 (2014): 620–626, https://doi.org/10.3182/20140313-3-IN-3024.00079.

6. V. T. Minh, T. Mart, R. Moezzi, and M. Juurma, "Performances of PID and Different Fuzzy Methods for Controlling a Ball on Beam," *Open Engineering* 6, no. 1 (2016), https://doi.org/10.1515/eng-2016-0018.

7. I. M. Mehedi, U. M. Al-Saggaf, R. Mansouri, and M. Bettayeb, "Two Degrees of Freedom Fractional Controller Design: Application to the Ball and Beam System," *Measurement* 135 (2019): 13–22, https://doi.org/10.1016/j.measurement.2018.11.021.

8. M. Ding, B. Liu, and L. Wang, "Position Control for Ball and Beam System Based on Active Disturbance Rejection Control," *Systems Science & Control Engineering* 7, no. 1 (2019): 97–108, https://doi.org/10.1080/21642583.2019.1575297.

9. P. Aryan, V. Kumar, G. L. Raja, T. R. Chelliah, and Y. V. Hote, "Robust Shifted-IMC Based Modified Decoupled Smith Predictor for Delay-dominant Integrating-type Chemical Processes," *International Journal of Systems Science* Early View (2025): 1–19.

10. D. Mukherjee, G. Lloyds Raja, P. Kundu, and A. Ghosh, "Analysis of Fractional Calculus-Based MRAC and Modified Optimal FOPID on Unstable FOPTD Processes," in *Modeling, Simulation and Optimization: Proceedings of CoMSO 2021*, eds. S. Kumar, F. P. G. Márquez, A. K. Singh, and A. Mahajan, Smart Innovation, Systems and Technologies. 293 (Springer, 2022), 427–442.

11. D. Mukherjee, G. L. Raja, P. Kundu, and A. Ghosh, "Fractional Standalone Backstepping Control for Nonlinear Continuous Stirred Tank Reactor," *International Journal of Robust and Nonlinear Control* 35, no. 17 (2025): 7422–7437, https://doi.org/10.1002/rnc.70058.

12. D. Das, S. Chakraborty, D. Kumar, and G. L. Raja, "Dual-loop PID Control Strategy for Ramp Tracking and Ramp Disturbance Handling for Unstable CSTRs," *Chemical Product and Process Modeling* 19, no. 6 (2024): 967–987, https://doi.org/10.1515/cppm-2024-0081.

13. G. L. Raja, "Robust I-PD Controller Design With Case Studies on Boiler Steam Drum and Bioreactor," in *Proceedings of the 2023 15th International Conference on Computer and Automation Engineering (ICCAE)*, (IEEE, 2023), 486–491, https://doi.org/10.1109/ICCAE56788.2023.10111205.

14. A. Sagar, R. Radhakrishnan, and G. L. Raja, "Cascade plus Feed-forward Control Strategy for Enhanced Regulation in Maglev System," *IFAC-PapersOnLine* 57 (2024): 355–360, https://doi.org/10.1016/j.ifacol.2024.05.061.

15. Shamsuzzoha, M., Lloyds Raja, G. eds., *PID Control for Linear and Nonlinear Industrial Processes* (IntechOpen, 2023).

16. P. Aryan and G. L. Raja, "Equilibrium-Optimized IMC-PD Double-Loop Control Strategy for Industrial Processes With Dead Time," in *PID Control for Linear and Nonlinear Industrial Processes*, eds. M. Shamsuzzoha and G. L. Raja, (IntechOpen, 2023), 37–50.

17. S. S. Ali, "Position Control of Ball and Beam System Using Robust h∞ Loop Shaping Controller," *Indonesian Journal of Electrical Engineering and Computer Science* 19, no. 1 (2020): 91, https://doi.org/10.11591/ijeecs.v19.i1.pp91-98.

18. S. Zaare and M. R. Soltanpour, "The Position Control of the Ball and Beam System Using State-disturbance Observe-based Adaptive Fuzzy Sliding Mode Control in Presence of Matched and Mismatched Uncertainties," *Mechanical Systems and Signal Processing* 150 (2021): 107243, https://doi.org/10.1016/j.ymssp.2020.107243.

19. Y. Sahu, B. Gupta, M. Wael, and R. Shalaby, "Optimal PD-PD and State Feedback Control of Underactuated Ball and Beam System With Uncertainty and Disturbances," in *Mathematical Modeling in Physical Sciences*, ed. D. T. Tsahalis, Lecture Notes in Networks and Systems. 954 (Springer, 2024), 87–104.

20. R. Raj, "PID-Based Optimized Fuzzy Controller Design for Ball and Beam System," in *Proceedings of the 2024 5th International Conference on Recent Trends in Computer Science and Technology (ICRTCST)*, (IEEE, 2024), 245–249, https://doi.org/10.1109/ICRTCST61793.2024.10578440.

21. H. Al-Khazraji, K. Albadri, R. Almajeez, and A. Humaidi, "Synergetic Control-Based Sea Lion Optimization Approach for Position Tracking Control of Ball and Beam System," *International Journal of Robotics and Control Systems* 4, no. 4 (2024): 1547–1560.

22. A. H. Issa, S. A. Mahmood, A. T. Humod, and N. M. Ameen, "Robustness Enhancement Study of Augmented Positive Identification Controller by a Sigmoid Function," *IAES International Journal of Artificial Intelligence (IJ-AI)* 12, no. 2 (2023): 686, https://doi.org/10.11591/ijai.v12.i2.pp686-695.

23. E. Çelik, "Exponential PID Controller for Effective Load Frequency Regulation of Electric Power Systems," *Isa Transactions* 153 (2024): 364–383.

24. L. Abualigah, D. Izci, S. Ekinci, and R. A. Zitar, "Optimizing Aircraft Pitch Control Systems: A Novel Approach Integrating Artificial Rabbits Optimizer With PID-F Controller," *International Journal of Robotics and Control Systems* 4, no. 1 (2024): 354–364, https://doi.org/10.31763/ijrcs.v4i1.1347.

25. W. Zhao, L. Wang, Z. Zhang, S. Mirjalili, N. Khodadadi, and Q. Ge, "Quadratic Interpolation Optimization (QIO): A New Optimization Algorithm Based on Generalized Quadratic Interpolation and Its Applications to Real-World Engineering Problems," *Computer Methods Applied Mechanics and Engineering* 417 (2023): 116446, https://doi.org/10.1016/j.cma.2023.116446.

26. D. Izci, S. Ekinci, E. Çelik, M. Bajaj, V. Blazek, and L. Prokop, "Dynamic Load Frequency Control in Power Systems Using a Hybrid



17518652, 2026, 1, Downloaded from https://ietresearch.onlinelibrary.wiley.com/doi/10.1049/cth2.70107 by Turkey Cochrane Evidence Aid, Wiley Online Library on [12/01/2026]. See the Terms and Conditions (https://onlinelibrary.wiley.com/terms-and-conditions) on Wiley Online Library for rules of use; OA articles are governed by the applicable Creative Commons License

Simulated Annealing Based Quadratic Interpolation Optimizer," *Scientific Reports* 14, no. 1 (2024): 26011, https://doi.org/10.1038/s41598-024-77247-3.

27. A. S. A. Bayoumi, R. A. El Sehiemy, M. El-Kemary, and A. Abaza, "Advanced Extraction of PV Parameters' Models Based on Electric Field Impacts on Semiconductor Conductivity Using QIO Algorithm," *Scientific Reports* 14, no. 1 (2024): 15397, https://doi.org/10.1038/s41598-024-65091-4.

28. F. Dao, Y. Zeng, Y. Zou, and J. Qian, "Fault Diagnosis Method for Hydropower Unit via the Incorporation of Chaotic Quadratic Interpolation Optimized Deep Learning Model," *Measurement* 237 (2024): 115199, https://doi.org/10.1016/j.measurement.2024.115199.

29. S. Ekinci, D. Izci, V. Gider, L. Abualigah, M. Bajaj, and I. Zaitsev, "Efficient Control Strategy for Electric Furnace Temperature Regulation Using Quadratic Interpolation Optimization," *Scientific Reports* 15, no. 1 (2025): 154, https://doi.org/10.1038/s41598-024-84085-w.

30. E. Khajavi, A. R. Taghavi Khanghah, and A. Javadzade Khiavi, "An Efficient Prediction of Punching Shear Strength in Reinforced Concrete Slabs Through Boosting Methods and Metaheuristic Algorithms," *Structures* 74 (2025): 108519, https://doi.org/10.1016/j.istruc.2025.108519.

31. N. B. Almutairi and M. Zribi, "On the Sliding Mode Control of a Ball on a Beam System," *Nonlinear Dynamics* 59, no. 1–2 (2010): 221–238, https://doi.org/10.1007/s11071-009-9534-8.

32. M. Abdel-Basset, R. Mohamed, M. Jameel, and M. Abouhawwash, "Spider Wasp Optimizer: A Novel Meta-heuristic Optimization Algorithm," *Artificial Intelligence Review* 56, no. 10 (2023): 11675–11738, https://doi.org/10.1007/s10462-023-10446-y.

33. S. Suyanto, A. A. Ariyanto, and A. F. Ariyanto, "Komodo Mlipir Algorithm," *Applied Soft Computing* 114 (2022): 108043, https://doi.org/10.1016/j.asoc.2021.108043.

34. A. Mohammadi-Balani, M. Dehghan Nayeri, A. Azar, and M. Taghizadeh-Yazdi, "Golden Eagle Optimizer: A Nature-inspired Meta-heuristic Algorithm," *Computers & Industrial Engineering* 152 (2021): 107050, https://doi.org/10.1016/j.cie.2020.107050.

35. S. Li, H. Chen, M. Wang, A. A. Heidari, and S. Mirjalili, "Slime Mould Algorithm: A New Method for Stochastic Optimization," *Future Generation Computer Systems* 111 (2020): 300–323, https://doi.org/10.1016/j.future.2020.03.055.

36. T. M. Shami, A. A. El-Saleh, M. Alswaitti, Q. Al-Tashi, M. A. Summakieh, and S. Mirjalili, "Particle Swarm Optimization: A Comprehensive Survey," *IEEE Access* 10 (2022): 10031–10061, https://doi.org/10.1109/ACCESS.2022.3142859.

37. S. Katoch, S. S. Chauhan, and V. Kumar, "A Review on Genetic Algorithm: Past, Present, and Future," *Multimedia Tools and Application* 80, no. 5 (2021): 8091–8126, https://doi.org/10.1007/s11042-020-10139-6.

38. R. Storn and K. Price, "Differential Evolution—A Simple and Efficient Heuristic for Global Optimization Over Continuous Spaces," *Journal of Global Optimization* 11, no. 4 (1997): 341–359, https://doi.org/10.1023/A:1008202821328.

39. M. Jabari, D. Izci, S. Ekinci, M. Bajaj, and I. Zaitsev, "Performance Analysis of DC-DC Buck Converter With Innovative Multi-stage PIDn(1+PD) Controller Using GEO Algorithm," *Scientific Reports* 14, no. 1 (2024): 25612, https://doi.org/10.1038/s41598-024-77395-6.

40. M. Jabari, S. Ekinci, D. Izci, M. Bajaj, V. Blazek, and L. Prokop, "Efficient Pressure Regulation in Nonlinear Shell-and-tube Steam Condensers via a Novel TDn(1 + PIDn) Controller and DCSA Algorithm," *Scientific Reports* 15, no. 1 (2025): 2090, https://doi.org/10.1038/s41598-025-86107-7.

41. A. P. Loh, X. Cai, and W. W. Tan, "Auto-tuning of Phase Lead/Lag Compensators," *Automatica* 40, no. 3 (2004): 423–429, https://doi.org/10.1016/j.automatica.2003.10.009.

42. D. Izci, S. Ekinci, E. Eker, and A. Demirören, "Multi-strategy Modified INFO Algorithm: Performance Analysis and Application to Functional Electrical Stimulation System," *Journal of Computational Science* 64 (2022): 101836, https://doi.org/10.1016/j.jocs.2022.101836.



17518652, 2026, 1, Downloaded from https://ietresearch.onlinelibrary.wiley.com/doi/10.1049/cth2.70107 by Turkey Cochrane Evidence Aid, Wiley Online Library on [12/01/2026]. See the Terms and Conditions (https://onlinelibrary.wiley.com/terms-and-conditions) on Wiley Online Library for rules of use; OA articles are governed by the applicable Creative Commons License